




Mitoxantrone in Synergism with Gold Hexagonal Nanoparticles and Gamma Radiation for Effective Treatment of MCF7 Cells

Wael Darwish¹; Rowad A Lafta²; Medhat Wahba Shafaa³; Mohamed S. El-Nagdy⁴

¹ Department of Polymers and Pigments, National Research Centre, Dokki, Giza, Egypt. 

² Physics Department, Faculty of Science, Helwan University, Cairo, Egypt.

³ Physics Dept., Medical Biophysics Division Faculty of Science Helwan University

⁴ Physics Department, Faculty of Science, Helwan University, Cairo, Egypt

Abstract

Biocompatible cross-linked chitosan nanoparticles comprising the cancer chemotherapeutic drug (mitoxantrone, MX) and the novel radiosensitizer hexagonal gold nanoparticles (HG) were prepared and characterized. The prepared nanoparticles were applied, in synergism with external γ -radiation, as dual (chemo-radio) model for treatment of human breast cancer cell (MCF-7). In vitro studies revealed that HG significantly enhances the response of MCF-7 to low and moderate doses of γ -radiation (2 and 4 Gy). Cell viability assay demonstrated the synergistic anticancer actions of mitoxantrone chemotherapy and gold-sensitized γ -radiation therapy. The prepared combinatorial model is potential for efficient and safer treatment of MCF7 cancer cells.

Key words: Hexagonal gold, chitosan nanoparticles, mitoxantrone, MCF-7, radiotherapy.

1. Introduction

Combined therapeutic modalities have been recently developed to overcome the problems related to the increasing number of multi-drug resistive cancer cells. In such modalities, two or more therapeutics of different modes of action are incorporated in a formulation. When a combined therapeutic formulation is designed, moderate release kinetics and synergistic cytotoxic effects of both drugs are the key parameters. Polymeric nanoparticles, especially those of natural origin are highly preferred as nanocarriers in multidrug therapeutic models because of their biocompatibility and biodegradability [1]. Chitosan nanoparticles are characterized with ease of preparation, high drug entrapment, sustained drug release and high cellular uptake rates [2,3]. Combined (chemo-radio) therapy is one of the most effective dual therapeutic models for cancer treatment [4,5]. In this model, a radiosensitizer is incorporated with a chemotherapeutic drug in a well-designed nanoformulation. The use of radiosensitizers as an effective tool to enhance the radiotherapy potency against radiation resistance of hypoxic tumor cells [6]. Generally, gold nanoparticles (GNPs) exhibit strong X-ray or gamma-ray attenuation capability and therefore can be used as a radiosensitizer to localize the radiation energy in tumors and enhance the radiotherapeutic efficiency [7]. The high sensitization enhancement ratios (SERs) of GNPs is

attributed to their strong photoelectric absorption coefficient [8]. In addition, GNPs are widely used as radiosensitizers due to their biocompatibility, ease of synthesis and high cellular internalization. Different shapes of gold nanoparticles, such as spheres, rods, and spikes exhibited different radiosensitizing effects depending on the ability of cellular internalization [9,10]. Fathy et al. [11a] reported in high cytotoxicity of CS-GNPs-DOX accompanied by different doses of X-rays (0.5, 1 and 3 Gy) against breast cancer cells (MCF-7). Combined (chemo-radio) therapeutic model comprising tirapazamine conjugated GNPs proved synergistic anticancer actions against HepG2 cells [11b]. On the other side, mitoxantrone is an anthracenedione-based chemotherapeutic that can intercalate into DNA and acts as topoisomerase II inhibitor [12]. Mitoxantrone is effectively used for treatment of breast cancer, leukemia, and lymphoma. The ultimate goal of this work was to prepare chitosan nanoparticles loaded with mitoxantrone and/or hexagonal gold nanoparticles. The key parameter in this formulation was to put mitoxantrone nanoparticles in synergism with hexagonal gold nanoparticles (HG) and gamma radiation as a combinatorial (chemo-radio) therapeutic model potential for treatment of MCF-7 cells. Hexagonal gold nanoparticles are expected to enhance the response of MCF-7 cells to the ionizing radiation at different doses.

*Corresponding author e-mail: waeldarwin78@yahoo.com; (W. Darwish)

EJCHEM use only: Receive Date: 15 July 2021, Revise Date: 27 July 2021, Accept Date: 12 September 2021

DOI: [10.21608/ejchem.2021.86310.4185](https://doi.org/10.21608/ejchem.2021.86310.4185)

©2022 National Information and Documentation Center (NIDOC)

2. Experimental section

2.1 Materials

Chitosan (CAS 9012-76-4) low viscosity from shrimp shells, chloroauric acid ($\text{HAuCl}_4 \cdot 4\text{H}_2\text{O}$, 99.99%), sodium tripolyphosphate (TPP), poly(ethylene glycol) methyl ether thiol (mPEG-SH) ($M_w = 6000$), mitoxantrone hydrochloride (MX) (99%) were products of Sigma (Merck), Germany. Chitosan (CS) was refined twice by dissolving in 0.1% AcOH, filtered, reprecipitated by dropping of 20 N aqueous sodium hydroxide, filtered again and finally dried under reduced pressure [13]. D-(+)-Glucono-1,5-lactone was a product of Alfa Aesar (CAS: 90-80-2). Milli-Q water was used for the preparation of the final formulations, otherwise deionized water was used.

2.2 Instruments

Transmission electron microscope (TEM) images were recorded on a JEM-2100, Jeol electron microscope. Chitosan polymeric nanoparticles were clearly visualized by staining with phospho-tungestic acid. Dynamic light scattering (DLS) instrument (PSS, Santa Barbara, CA, USA), using the 632 nm line of a He-Ne laser as the incident light with angle 90° and zeta potential with external angle 18.9° . Optical extinction spectra were recorded at room temperature using a computerized Cary 300 spectrophotometer, Agilent Technologies, over a spectral range between 400 and 1000 nm and a spectral resolution of 2 nm. Differential scanning calorimetry DSC131 evo (SETARAM Inc., France) was used to perform the differential scanning calorimeter analysis, Nanomaterial Investigation laboratory, Central Laboratories Network, National Research Centre (NRC), Egypt. The instrument was calibrated using the standards (Mercury, Indium, Tin, Lead, Zinc and Aluminum). Nitrogen and Helium were used as the purging gases. The test was programmed including the heating zone from 25°C to 300°C with a heating rate $10^\circ\text{C} / \text{min}$. The samples were weighed in aluminum crucible 120 μL and introduced to the DSC. The thermogram results were processed using (CALISTO Data processing software v.149).

2.3 Methods

2.3.1 Preparation of hexagonal gold nanoparticles (HG)

These gold nanoblocks were prepared according to procedures reported in our previous work [14]. In brief, a solution of 1% concentration of D-(+)-Glucono-1,5-lactone was prepared by dissolving in Milli-Q ultrapure water $18.2 \text{ M}\Omega \cdot \text{cm}$. Chitosan was dissolved in this solution to obtain a final chitosan concentration of 0.05%, w/v. The solution was filtered through a microfilter (0.45 μm) and brought

to boiling before addition of $\text{HAuCl}_4 \cdot 3\text{H}_2\text{O}$ (200 μL , 49 mg/mL). The color of the solution turns into ruby red color after 10 minutes. The solution was cooled to room temperature and the gold hexagonal nanoparticles were separated by centrifugation (13,000 rpm, 4°C). Purification was carried out by successive processes of sonication in pure water and centrifugation. PEGylated hexagonal gold nanoparticles were prepared by addition of mPEGSH 3 (mg) to the aqueous gold solution followed by sonication for 1 h. Excess mPEGSH was removed by centrifugation. PEG-stabilized HG was redispersed in ultrapure water. The plasmonic peak of HG colloid at $\lambda_{\text{max}} = 536 \text{ nm}$ showed no shift or broadening after storage in dark at 4°C for more than one month. The stability of HG colloid may be attributed to lactone and polymeric coats on the surface of the particles.

2.3.2 Preparation of chitosan nanoparticles (CSNPs)

Biocompatible CSNPs were prepared by the ionic gelation method using TPP as a cross linker. Chitosan was dissolved in AcOH (1% w/v) to give a final CS concentration of 0.1%. Aqueous NaOH solution (20 N) was used to raise the pH of the solution to 4.8. For preparation of empty CS NPs, TPP solution (1%) was added slowly till opalescence solution is observed. After stirring for 3 h, the NPs were separated by centrifugation (10,000 rpm, 10 min). CS NPs were purified by successive sonication in deionized water and centrifugation. NPs were redispersed in ultrapure water and freeze-dried till characterization. Loading of MX, HG, or both in CS NPs was achieved by dissolving MX and/or HG in CS solution before addition of TPP. Our preliminary studies optimized the reaction conditions to obtain CS NPs of the desired size, surface potential and loading efficiency.

2.3.3 Morphological properties of the nanoparticles

2.3.4 Drug-loading and encapsulation efficiency (EE)

The supernatant collected from repetitive washing of the NPs during the synthesis procedure was collected, neutralized to $\text{pH}=7.2$ and analyzed for the unloaded (free) amounts of HG and MX. Thus, the loaded amounts of HG and MX can be calculated by abstracting the unloaded amounts from the total added amounts. Concentration of gold in the supernatant was determined using atomic absorption spectroscopy as described elsewhere [9]. Concentration of mitoxantrone was determined via spectroscopic method by monitoring the absorption of (MX) at 610 nm [15]. Drug loading (DL, %) and entrapment efficiency (EE, %) were calculated according to equations 1-2, where (Cs) is the

concentration of HG or MX in the supernatant and the total concentration of each species (Ct).

$$\text{Drug Loading (\%)} = \frac{C_t - C_s}{\text{Weight of the NPs powder}} \times 100$$

$$\text{Encapsulation Efficiency (\%)} = \frac{C_t - C_s}{C_t} \times 100$$

2.3.5 In vitro release profile of mitoxantrone

The release profile of mitoxantrone from the nanoparticles was carried out according to the standard method reported in literature [15]. In brief, 50 mg of the lyophilized nanoparticles was dissolved in 10 ml of PBS (pH 7.4) and placed in dialysis tubing (12-14 KDa). The dialysis tubes were tied from both sides and gently placed in a container containing an aqueous media at 37 °C in a shaker incubator. At different time intervals ranging from 1 to 72 h, 3 mL of the dialysate was drawn out and analyzed for mitoxantrone by the same spectrophotometric method used in the previous section. Another 3 mL of PBS was added to the dialysate to compensate the drawn amount. The cumulative release was then calculated.

2.3.6 Cell viability assay

MCF-7 cells were obtained from American Type Culture Collection and were cultured using DMEM (Invitrogen/Life Technologies) supplemented with 10% FBS (Hyclone), 10 µg/mL of insulin (Sigma), and 1% penicillin-streptomycin. Cultures were maintained at 37 °C in a humidified 5% CO₂ sterile incubator. All of the other chemicals and reagents were from Sigma, or Invitrogen. Cells were seeded in 96-well plates with a density of (1.2-1.8 × 10³) cells/well and were incubated at 37 °C for 24 h. Cells were treated with serial concentrations of the formulations to be tested and incubated at 37 °C for 48 h before MTT assay. Sterile formulations were obtained by autoclaving (121 °C, 20 min), since chitosan nanoparticles are stable under these autoclaving conditions [16,17].

2.3.7 Cells irradiation

After incubation of the cells for 48 h, the media was replaced with fresh media and the cells were irradiated with different radiation doses (2 and 4 Gy) by cesium-137 source and incubated at 37 °C. The source-to-cell surfaces distance was adjusted at 100 cm for the irradiated culture plates at a radiation field size of 15×15 cm². Twenty four hours post irradiation, cell viability was assessed by incubating the cells for 2 h with a medium containing neutral red solution. After replacing the media several times, the dye in each well was extracted and the absorbance at

a wavelength of 570 nm was read using a plate reader (Victor 3V-1420, Finland). Sensitization enhancement ratio (SERs) of various treatment groups was calculated and compared using human breast cancer cell line (MCF-7). (SER) was calculated by dividing the surviving fraction of the irradiated cells in the absence of gold on the surviving fraction in presence of gold for each dose of radiation according to the standard protocols [18].

2.3.8 Statistical analysis

All experiments were repeated three times (n = 3) and differences in the data were evaluated with one way ANOVA test. The data are given as a mean ± SD at statistically significant values (P < 0.05).

3. Results and discussions

3.1 Hexagonal gold nanoparticles

D-(+)-glucono-1,5-lactone was used to dissolve chitosan instead of acetic acid. Afterwards, chitosan solution was used to reduce Au³⁺ ions producing lactone-capped hexagonal nanoparticles (HG). The ruby-red color of colloidal gold is characteristic for the excitation of surface plasmonic resonance of gold nanoparticles and was verified by UV-Vis extinction (absorbance plus scattering) spectroscopy measurements (Fig. 1A). The extinction spectrum of lactone-capped hexagonal gold nanoparticles presents a maximum at 536 nm. PEGylation of the prepared GNPs was carried out to enhance the physiological stability of the plasmonic nanoparticles [5]. Transmission electron microscopy presents hexagonal-shaped nanoparticles of mean diameter of 28 nm (Fig. 1B). Dynamic light scattering (DLS) measurements showed nearly monodispersed nanoparticles of a mean hydrodynamic radius of 34.2± 3.5 nm. Zeta potential measurements of HG nanoparticles in its colloid showed a negative surface potential of -14.62± 4 mV (Table 1). The negative surface potential confirms the lactone capping instead of chitosan capping of the gold nanoparticles. The formation of hexagonal crystals of gold instead of the well-known spherical nanoparticles may be attributed to the presence of D-(+)-glucono-1,5-lactone which increases the viscosity of the crystal growth environment and act as a capping agent of the produced crystalline nanoparticles. We have previously developed this novel synthetic procedure in our group. This procedure is more biocompatible than the surfactant-based method [19] and more facile than the previously given procedures [10,20]. We also aimed to evaluate the efficacy of the hexagonal gold nanoparticles as novel radiosensitizers.

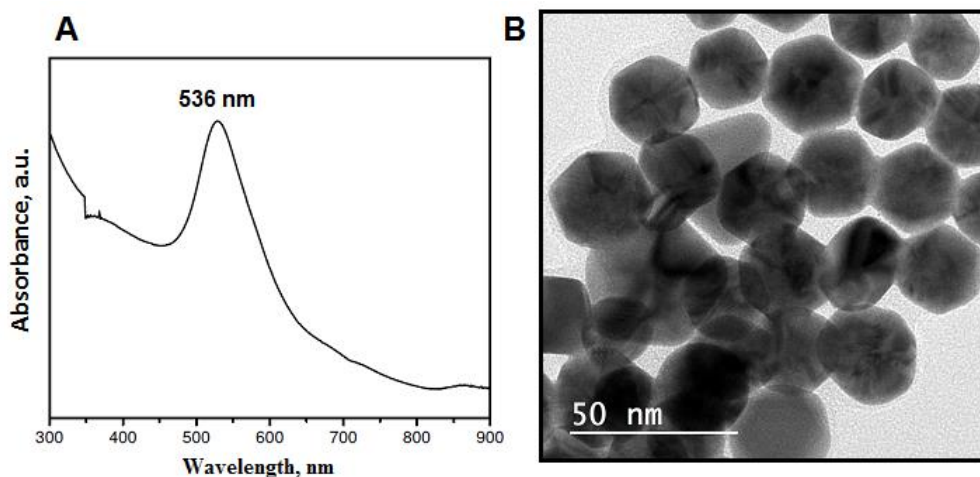


Fig. 1. Extinction spectra of hexagonal GNPs (A) and TEM images of HG NPs (B).

3.2 Chitosan nanoparticles

In this work, stable colloid of chitosan nanoparticles incorporating HG nanoparticles and/or mitoxantrone were prepared by the ionic gelation method using tripolyphosphate (TPP) as a non-toxic polyanion counter-ion [21]. The conditions were optimized in our laboratory to yield nearly monodispersed nanoparticles with high drug payload (Table 1). The physicochemical properties of the prepared nanoparticles were characterized by TEM, DLS, zeta-potential analyzer and DSC. TEM images of all CS NPs showed regular and spherical shaped nanoparticles. The size distribution profiles (Table 1) present nanoparticles with a mean diameter of 165.2 ± 2.2 , 190.2 ± 3.7 and 196.6 ± 4.8 nm, for CS-MX, CS-HG and CS-MX-HG NPs, respectively. All CS NPs showed a narrow size distribution (polydispersity index <1) and positive zeta potential (Table 1). Generally, CS-MX nanoparticles have hydrodynamic radius lower than that of CS-HG and CS-MX-HG nanoparticles. This may be attributed to

the relatively large size of HG nanoparticles compared to MX nanoparticles.

DSC measurements of pure mitoxantrone hydrochloride (MX), chitosan polymer, empty CSNP, CS-MX NPs and CS-MX-HG NPs were carried out to identify the possible interactions between the drug and other constituents (Table 2). DSC thermogram of pure mitoxantrone hydrochloride showed a sharp endothermic peak at 203.9 °C indicating the melting temperature (T_m) of the pure drug. In the thermogram of chitosan polymer the endothermic peak at 153.6 °C is in accordance with the literature [22]. TPP showed the well known endothermic peak at 135.9 °C. Unloaded CS NPs had two endothermic peaks at 152.4 and 218.4 °C [23]. The absence of the melting peak of MX in the DSC thermogram of CS-MX NPs and CS-MX-HG NPs indicates the amorphous nature of the drug nanoparticles in the nanoparticles [24].

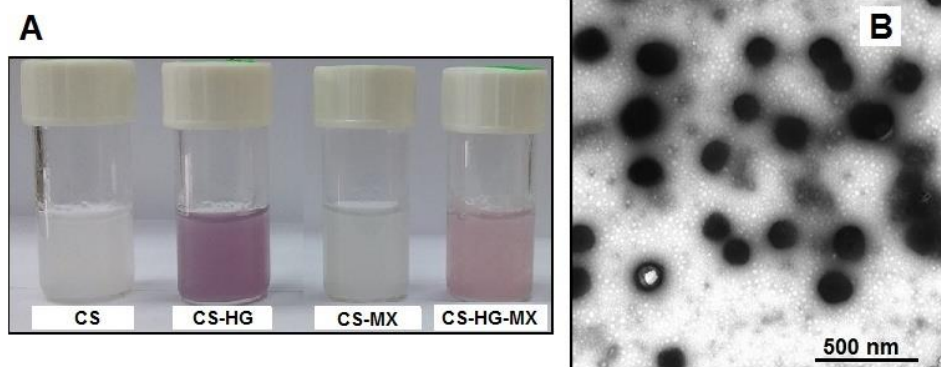


Fig. 2. Photographs of the as-synthesized CS nanoparticles (A), and TEM image of MX and HG-loaded CS nanoparticles (B).

Table 1. Physicochemical properties of the prepared HG nanoparticles and CS nanoparticles. The data corresponds to the average of five independent batches and are presented as mean \pm SD

Formulation	HD \pm SD (nm)	PDI \pm SD	Zeta \pm SD (mV)	EE (%)	
				HG	MX
HG NPs	34.11 \pm 1.8	0.425	- 14.62 \pm 2.1	----	----
Empty CS NPs	155.28 \pm 4.5	0.322	29.33 \pm 1.9	----	----
CS-HG NPs	190.2 \pm 3.7	0.342	22.15 \pm 1.4	65.4 \pm 3.4	----
CS-MX NPs	165.2 \pm 2.2	0.286	15.44 \pm 0.6	----	23.6 \pm 1.8
CS-HG-MX NPs	196.6 \pm 4.8	0.365	16.96 \pm 1.4	51.8 \pm 4.5	18.5 \pm 1.7

Note: Data represent the mean \pm SE; n=3. Abbreviations CS: chitosan; EE: encapsulation efficiency; HD: hydrodynamic radius estimated by DLS; HG: Hexagonal gold nanoparticles; MX: mitoxantrone hydrochloride; PDI: polydispersity index; SD: standard deviation; Zeta: zeta potential.

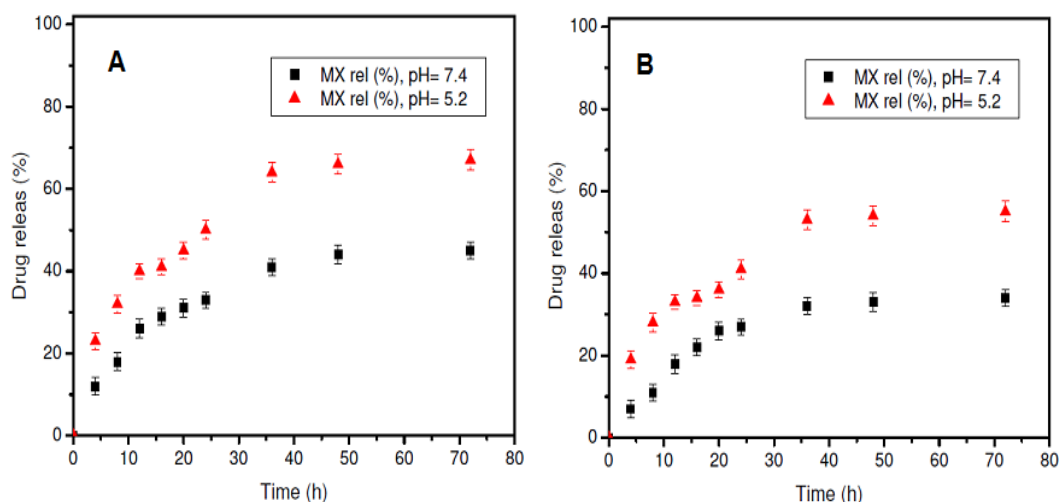
Table 2. The endothermic processes representing the melting temperatures (T_m) of pure MX, chitosan, TPP, empty CS NPs, CS-MX and CS-MX-HG NPs

Sample	T _m (°C)
Pure MX	203.9
CS polymer	153.6
CS NPs	152.4; 218.4
TPP	135.9
CS-MX NPs	138.2; 154.1; 216.4
CS-MX-HG NPs	134.9; 156.3; 222.1

3.3 In vitro release profile

The prepared nanofomulations exhibited a prolonged biphasic release for both HG and mitoxantrone within 72 h (Fig. 3). A similar release profile was reported

for both chitosan and lactic acid grafted-chitosan nanoparticles [25]. The amount of released MX is greater at acidic pH (5.2) than in neutral pH (7.4). This release mechanism is adequate for cancer treatment due to the well known acidic extracellular tumor environment [26,27]. It was suggested that in the acidic condition, the glucose amino group in chitosan chain bonded with H⁺ to form NH⁺ and dissolved in the medium rapidly, thus accelerating the breaking down of particle structure and resulting in fast diffusion of the drug from the interior of NPs [28]. The percent of released MX from CS-MX NPs after 48 h were found to be about 45 and 67 % in neutral and acidic medium, respectively. Lower amounts were observed from CS-MX-HG NPs (34 and 55 % in neutral and acidic medium, respectively). This behavior may be attributed to physical bonding of some mitoxantrone molecules to the surface of gold hexagonal nanoparticles.

**Fig. 3. In vitro release kinetics of MX from CS-MX (A) and CS-MX-HG (B) in neutral and acidic media.**

3.4 In vitro radiosensitization

In a previous work [14], we estimated the sensitization enhancement ratios (SER) of hexagonal gold nanoparticles by colony formation assay. The sensitization enhancement ratio (SER) of aqueous hexagonal gold nanoparticles was found to be 1.44.

This value is slightly lower than that of gold nanospheres (1.62) but higher than that of nanospikes and nanorods were estimated to be (1.37 and 1.21, respectively [29]. SERs of gold nanoparticles depends on the cellular uptake which in

turn depends on size, shape and nature of coating [30].

3.5 *In vitro* anticancer efficiency

The cytotoxic effects of the prepared HG and chitosan formulations were studied by treating human breast cancer cells (MCF-7) with the prepared formulations followed by γ -irradiation with different doses (0, 2, and 4Gy) (Fig. 4). MTT assay results are shown in Figs. 5. According to the *in vitro* release profile of the prepared formulations (Fig. 3), incubation time of 48 h was chosen for all cell line experiments aiming to achieve optimum release of both MX and HG. Previous studies reported on IC₅₀ value of 0.42 μ M for free mitoxantrone against MCF-7 cells [31]. Therefore, we used in this work different concentrations of mitoxantrone in the range of (50-300 μ M) to be tested considering the incomplete release of MX from CSNPs. The corresponding concentrations of gold in the as-prepared formulations were in the range of (5.2 -32.4 μ M).

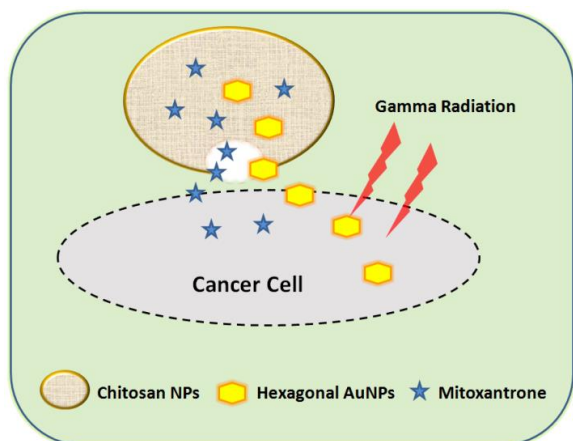


Fig. 4. Schematic illustration of synergistic (chemo-radio) killing effects on breast cancer cells.

3.5.1 Treatment without external radiation

The chemical cytotoxicity of the prepared formulations was tested against MCF-7 cells without external radiation. As seen in Fig. 5A, empty chitosan nanoparticles showed relatively high biocompatibility with cell viability percentage of about 90%. CS-MX nanoparticles showed considerable cytotoxicity in a dose-dependent manner. This is in accordance with the previous studies reported on an increment in cell cycle inhibition of cancer drugs when loaded in CSNPs [32]. It is well known that CS NPs are easily incorporated into the breast cancer cells and readily distributed in the cytoplasm after few hours of incubation [33]. On the other side, CS-HG NPs showed moderate chemical cytotoxicity indicating that HG could be efficiently released from CS NPs and internalized into MCF-7 cells via an endocytic

process. The chemical cytotoxicity of the model (CS-MX-HG) is significantly higher than that of both individual therapeutic indicating the synergistic chemotherapeutic effects of gold and MX. However, about 30 % of the cells could survive even at the highest concentrations of both MX and gold and therefore, irradiation step was carried out.

3.5.2 Irradiation experiments (Figs. 5B and 5C)

Figs. 5B and 5C showed that incubation of MCF-7 cells with empty CSNPs followed by irradiation with 2 Gy and 4 Gy reduced the cell viabilities to 47% and 38%, respectively. This reflects the significant response of MCF-7 cells to γ -radiation, compared to the cells treated only with empty CSNP without irradiation. Treatment with CS-MX followed by irradiation with 2 Gy and 4 Gy significantly reduced the cell viabilities more than values obtained after individual irradiation (Figs. 5B and 5C). This cytotoxicity markedly increases with increasing concentration of MX and also with increasing the radiation dose from 2 Gy to 4 Gy. This evidences the synergistic effects in the (chemo-radio) therapeutic model (CS-MX+ radiation). Figs (5B and 5C) showed the radiosensitization effect of hexagonal gold nanoparticles. For irradiation experiment, incubation with CS-MX-HG reduces the cell viabilities much more than incubation with CS-MX in all concentrations. It is obvious that, the optimum synergism and anticancer efficacy is achieved for NPs comprising MX and GNPs of concentrations, 300 and 32.4 μ M, respectively with subsequent radiation dose of 4 Gy (Fig. 5C). It can be concluded that HG can enhance the response of MCF-7 to the radiation in a concentration dependent manner. Eventually, this radiosensitization effect of HG is significant in concentration range of 16.2-32.4 μ M. These results confirm the effectiveness of the combined therapeutic model (CS-MX-HG) together with gamma radiation against human MCF-7 cells. This regimen can reduce the cell viability to less than 10% without need to elevated radiation dose (Figs 5B and 5C).

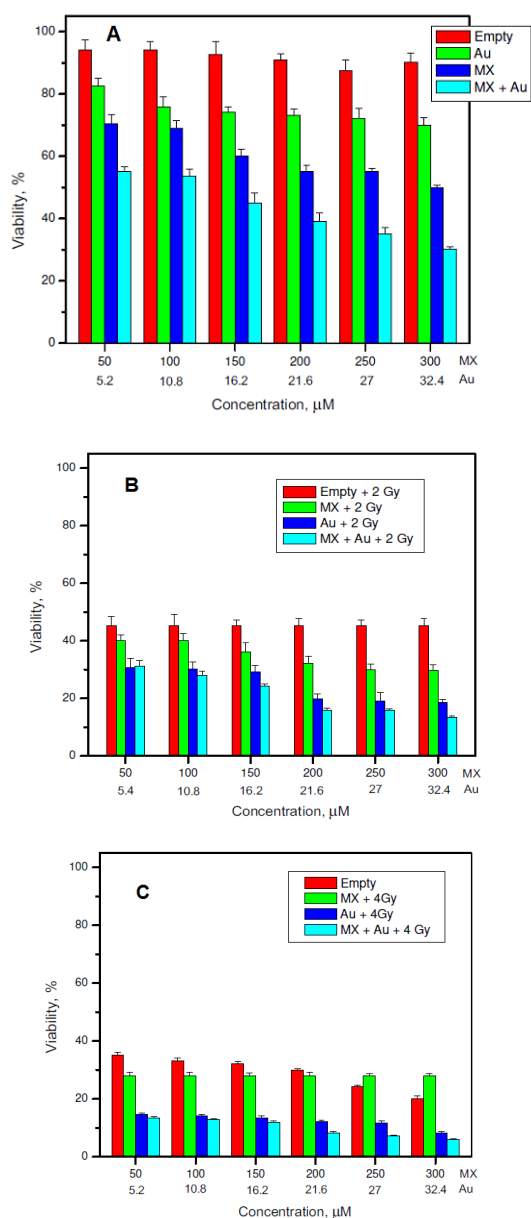


Fig. 5. The cytotoxicity results obtained by treating MCF-7 cell with the prepared formulations containing different concentrations of HG and MX followed by exposure to different radiation doses (0 Gy, A), (2 Gy, B) and (4 Gy, C).

4. Conclusions

Monodispersed chitosan nanoparticles comprising the cancer chemotherapeutic (mitoxantrone) and the novel radiosensitizer (hexagonal gold nanoparticles) were prepared. The multifunctional nanoparticles were characterized by small size, good drug entrapment and low polydispersity index. *In vitro* release kinetic studies revealed the sustained release of both mitoxantrone and gold from the nanoparticles with optimum release after 48 h. Formulations

comprising different concentrations of both MX and HG NPs were tested against human MCF-7 cells accompanied with different radiation doses (0, 2, 4Gy). CS-MX NPs showed moderate chemical cytotoxicity in the absence of external radiation. In presence of external radiation (2 or 4 Gy), the synergistic effects of CS-MX+R were clearly observed resulting in enhanced cytotoxicity higher than individual CS-MX NPs or radiation. Results also revealed that hexagonal gold nanoparticles are efficient radiosensitizers. It can be concluded that chitosan nanoparticles are suitable platforms capable to put mitoxantrone in synergism with gold hexagonal nanoparticles and gamma radiation for efficient treatment of human MCF7 cancer cells.

Acknowledgement

We are grateful for the financial support of (National Research Centre, Dokki, Giza, Egypt) within the In-house research project number 12020302.

Declaration of interest

The authors report no conflict of interest.

References

- [1] Liu T., Yang Y. and Chiang, W., Radiotherapy-controllable chemotherapy from ROS responsive polymeric nanoparticles for effective local dual modality treatment of malignant tumors. *Biomacromolecules*, **19**, 3825-3839(2018).
- [2] Pandya A., Qverbye A., et al., Drug-loaded photosensitizer-chitosan nanoparticles for combinatorial chemo- and photodynamic-therapy of cancer. *Biomacromolecules*, **21**, 1489-1498(2020).
- [3] Olmos, S., Roberto Díaz Torres, et al. Combinatorial use of chitosan nanoparticles, reversine, and ionizing radiation on breast cancer cells associated with mitosis deregulation. *Biomolecules*, **9**, 186-191(2019).
- [4] Shanei, A., Sazgarnia, A., et al., Dual function of gold nanoparticles in synergism with mitoxantrone and microwave hyperthermia against melanoma cells. *Asian Pac J Cancer Prev*, **18**, 2911-2917(2017).
- [5] Yoon J., Cho H., Hyo-Eon Jin H. and Maeng H. Mitoxantrone-loaded PEGylated gold nanocomplexes for cancer therapy. *J Nanosci Nanotechnol*, **19**, 687-690(2019).
- [6] Ningning M., Fu-Gen W. and Xiaodong Z., Shape-dependent radiosensitization effect of gold nanostructures in cancer radiotherapy: Comparison of gold nanoparticles, nanospikes, and nanorods. *ACS Appl Mater Interfaces*, **9**, 13037-13048(2017).
- [7] Zhang Y., Huang F., Ren C., et al., Enhanced radiosensitization by gold nanoparticles with acid-

- triggered aggregation in cancer radiotherapy. *Adv Sci*, **6**, 1801806(2019).
- [8] Butterworth K, McMahon S., Currellab F. and Prise, K., Physical basis and biological mechanisms of gold nanoparticle radiosensitization. *Nanoscale*, **4**, 4830-4838(2012).
- [9] Ningning M., Peidang L., Nongyue H., Ning G., Fu-Gen W. and Zhan C., Action of gold nanospikes-based nanoradiosensitizers: cellular Internalization, radiotherapy, and autophagy. *ACS Appl Mater Interfaces*, **9**, 31526-31542(2017).
- [10] Hu J., Wang Z. and Li J., Gold nanoparticles with special shapes: controlled synthesis, surface-enhanced raman scattering, and the application in biodetection. *Sensors*, **7**, 3299-3311(2007).
- [11] (A) Fathy M., Mohamed F., Elbially N. and Elshemey W., Multifunctional chitosan-capped gold nanoparticles for enhanced cancer chemoradiotherapy: An invitro study. *Physica Medica*, **48**, 76-83(2018). (B) Xi Liu, Yan Liu, Pengcheng Zhang, Xiaodong Jin, Xiaogang Zheng, Fei Ye, Weiqiang Chen, Qiang Li. The synergistic radiosensitizing effect of tirapazamine-conjugated gold nanoparticles on human hepatoma HepG2 cells under X-ray irradiation. *Int J Nanomed*, **11**, 3517-3531 (2016).
- [12] Patel K., Tre'dan O. and Tannock I., Distribution of the anticancer drugs doxorubicin, mitoxantrone and topotecan in tumors and normal tissues. *Cancer Chemother Pharmacol*, **72**, 127-138(2013).
- [13] Yong H., Xiqun J., Yin D., Haixiong G., Yuyan Y. and Changzheng, Y., Synthesis and characterization of chitosan-poly(acrylic acid) nanoparticles. *Biomaterials*, **23**, 3193-3201(2002).
- [14] Darwish et al. Unpublished results.
- [15] Jameela S. and Jayakrishnan A., Glutaraldehyde cross-linked chitosan microspheres as a long acting biodegradable drug delivery vehicle: studies on the *in vitro* release of mitoxantrone and *in vivo* degradation of microspheres in rat muscle. *Biomaterials*, **16**, 769-775(1995).
- [16] Kushwaha S., Rai A. and Sing S., Formulation of thermosensitive hydrogel containing cyclodextrin for controlled drug delivery of camptothecin. *Trop J Pharm Res*, **13**, 1007-1012(2014).
- [17] Qi L., Xu Z., Jiang X., Hu C. and Zou X., Preparation and antibacterial activity of chitosan nanoparticles. *Carbohydr Res*, **339**, 2693-2700(2004).
- [18] Hamzian N., Hashemi M. And Gorbani, M., *In-vitro* study of multifunctional plga-spion nanoparticles loaded with gemcitabine as radiosensitizer used in radiotherapy. *Iran J Pharm Res*, **18**, 1694-1703(2019).
- [19] Kuo C-H., Chiang T-F., Chen L-J. and Huang M.H., Synthesis of hiHGly faceted pentagonal- and hexagonal-shaped gold nanoparticles with controlled sizes by sodium dodecyl sulfate. *Langmuir*, **20**, 7820-7824(2004).
- [20] Peng P., Meng A., Braun M., Marshall A. and McIntyre P., Plasmons and inter-band transitions of hexagonal close packed gold nanoparticles. *Appl. Phys. Lett.*, **115**, 051107(2019).
- [21] Shafiei M., Jafarizadeh-Malmiri H. and Rezaei M., Biological activities of chitosan and prepared chitosan-tripolyphosphate nanoparticles using ionic gelation method against various pathogenic bacteria and fungi strains. *Biologia*, **74**, 1561-1568(2009).
- [22] Gomez-Burgaz M., Torrado G. and Torrado S., Characterization and superficial transformations on mini-matrices made of interpolymer complexes of chitosan and carboxymethylcellulose during *in vitro* clarithromycin release. *Eur J Pharm Biopharm*, **73**, 130-139(2009).
- [23] Sobhani Z., Samani S., Montaseri H. and Khezri E., Nanoparticles of chitosan loaded ciprofloxacin: fabrication and antimicrobial activity. *Adv Pharm Bull*, **7**, 427-432(2017).
- [24] Ilaiyaraja N., Devi A. and Khanum, F., Chlorogenic acid-loaded chitosan nanoparticles with sustained release property, retained antioxidant activity and enhanced bioavailability. *Asian J Pharm Sci*, **10**, 203-211(2015).
- [25] Bhattarai N., Ramay H., Chou S-H. and Zhang M., Chitosan and lactic acid-grafted chitosan nanoparticles as carriers for prolonged drug delivery. *Int J Nanomed*, **1**, 181-187(2006).
- [26] Ibrahim H., Farid O., Samir A. and Mosaad R. Preparation of chitosan antioxidant nanoparticles as drug delivery system for enhancing of anti-cancer drug. *Key Eng Mater*, **759**, 92-97(2018).
- [27] Prabakaran M., Chitosan-based nanoparticles for tumor-targeted drug delivery. *Int J biol macromol*, **72**, 1313-1322(2015).
- [28] Yu X., Hou J., Shi Y., Su C. and Zhao L., Preparation and characterization of novel chitosan-protamine nanoparticles for nucleus-targeted anticancer drug delivery. *Int J Nanomed*, **11**, 6035-6046(2016).
- [29] Chithrani D., Hgazani A. and Chan W., Determining the size and shape dependence of gold nanoparticle uptake into mammalian cells. *Nano Lett.*, **6**, 662-668(2006).
- [30] Zhang X., Luo Z., Chen J., Song S., Yuan X., Shen X., Wang H., Sun Y., Gao K., Zhang L., Fan S., Leong D., Guo M., Xie J., Ultrasmall glutathione-protected gold nanoclusters as next

generation radiotherapy sensitizers with hiHG tumor uptake and high renal clearance. *Sci Rep*, **5**, 8669–8675(2015).

- [³¹] Ji N., Yuan J., Jianjun Liu J. and Tian S., Developing multidrug-resistant cells and exploring correlation between BCRP/ABCG2 over-expression and DNA methyl-transferase. *Acta Biochim Biophys Sin*, **42**, 854-862(2010).
- [³²] Parveen S. and Sahoo S. Long circulating chitosan/PEG blended PLGA nanoparticle for tumor drug delivery. *Eur J pharmacol*, **670**, 372-383(2011).
- [33] Olmos S., Torres R., et al., Combinatorial use of chitosan nanoparticles, reversine, and ionising radiation on breast cancer cells associated with mitosis deregulation. *Biomolecules*, **9**, 186-191(2019).